UC San Diego
UC San Diego Previously Published Works

Title

Measurements of OCT Angiography Complement OCT for Diagnosing Early Primary Open-Angle Glaucoma

Permalink

https://escholarship.org/uc/item/1sf359s9

Journal

Ophthalmology Glaucoma, 5(3)

ISSN

2589-4234

Authors

Kamalipour, Alireza
Moghimi, Sasan
Jacoba, Cris Martin
et al.

Publication Date

2022-05-01

DOI

10.1016/j.ogla.2021.09.012

Peer reviewed

Measurements of OCTA Complement OCT for Diagnosing Early Primary Open Angle Glaucoma

Alireza Kamalipour, MD, MPH[1],[*], Sasan Moghimi, MD[1],[*], Cris Martin Jacoba, MD[1], Adeleh Yarmohammadi, MD[1], Kaileen Yeh, MD[1], James A. Proudfoot, MSc[1], Huiyuan Hou, MD, PhD[1], Takashi Nishida, MD, PhD[1], Ryan Caezar David, MD[1], Jasmin Rezapour, MD[1], Nevin El-Nimri, PhD[1], Robert N. Weinreb, MD[1]

[1]Hamilton Glaucoma Center, Shiley Eye Institute, Viterbi Family Department of Ophthalmology, University of California San Diego, La Jolla, CA.

Abstract

Purpose—To compare measurements of global and regional circumpapillary capillary density (cpCD) with retinal nerve fiber layer (RNFL) thickness, and characterize their relationship with visual function in early primary open-angle glaucoma (POAG).

Design—Cross-sectional study

Participants—Eighty healthy eyes, 64 pre-perimetric, and 184 mild POAG eyes from the Diagnostic Innovations in Glaucoma Study.

Methods—Global and regional RNFL thickness and cpCD measurements were obtained using optical coherence tomography (OCT) and OCT angiography (OCTA). For direct comparison at the individual and diagnostic group level, RNFL thickness and capillary density values were converted to a normalized relative loss scale.

Correspondence: Robert N. Weinreb, MD, Shiley Eye Institute, University of California, San Diego, 9500 Gilman Drive, La Jolla, CA 92093-0946. rweinreb@ucsd.edu.
[*]These authors had equal contributions as co-first authors.

Main Outcome Measures—RNFL thickness and cpCD normalized loss at the individual level and diagnostic group. Global and regional areas under the receiver operating characteristic curve (AUROC) for RNFL thickness and cpCD to detect pre-perimetric glaucoma and glaucoma. R-squared for the strength of associations between RNFL thickness-function and capillary density-function in diagnostic groups.

Results—Both global and regional RNFL thickness and cpCD decreased progressively with increasing glaucoma severity ($P<0.05$, except for temporal RNFL thickness). Global and regional cpCD relative loss values were higher than those of RNFL thickness ($P<0.05$) in pre-perimetric glaucoma (except for the superonasal region) and glaucoma (except for the inferonasal and superonasal regions) eyes. Race, IOP and cpCD were associated with greater cpCD than RNFL thickness loss in early glaucoma at the individual level ($P<0.05$). Global measurements of capillary density (whole image capillary density [wiCD] and cpCD) had higher diagnostic accuracies than RNFL thickness in detecting pre-perimetric glaucoma and glaucoma ($P<0.05$; except for cpCD/RNFL thickness comparison in glaucoma [$P=0.059$]). Visual function was significantly associated with RNFL thickness and cpCD globally and in all regions ($P<0.05$, except for temporal RNFL thickness-function association [$P=0.070$]).

Conclusions—Associations between capillary density and visual function were found in the regions known to be at highest risk for damage in pre-perimetric glaucoma eyes and all regions of mild glaucoma eyes. In early glaucoma, capillary density loss was more pronounced than RNFL thickness loss. Individual characteristics influence the relative magnitudes of capillary density loss compared to RNFL thickness loss. RNFL thickness and microvascular assessments are complementary and yield valuable information for the detection of early damages seen in POAG.

INTRODUCTION

Primary open angle glaucoma (POAG) is characterized by progressive loss of retinal ganglion cells and their axons, and accompanying damage to the visual field (VF).[1, 2] Early identification and subsequent treatment of glaucoma can prevent the development and progression of irreversible VF defects.[3] Spectral-domain optical coherence tomography (OCT) is used in clinical practice to detect quantitative structural changes of the optic disc and retinal nerve fiber layer (RNFL).[4-7] With optical coherence tomography angiography (OCTA) technology, there also is a decline in retinal microvascular density associated with glaucomatous injury to the optic nerve.[8, 9] Examining retinal microvasculature using OCTA has the potential to elucidate further the role of retinal microvascular changes in the development and progression of glaucoma.[10-13]

Retinal structural and microvascular alterations of the optic disc and retina have been proposed as factors associated with the development and progression of glaucomatous visual field damage.[13] However, questions regarding the temporality and relative magnitudes of structural and vascular change have not been fully answered. Most of the previous

studies evaluating these anatomical changes included a wide spectrum of disease severity where such changes have already been established.[12, 14] Identifying these changes in the early disease spectrum can potentially better address these questions and provide earlier differentiation between glaucomatous and healthy eyes.

Previous investigations have evaluated the diagnostic accuracy of different OCT parameters to discriminate healthy eyes from those with different severities of glaucomatous involvement.[15-31] Recently, studies have also assessed and compared the diagnostic accuracy of glaucoma detection of vessel density measured by OCTA to structural OCT parameters (such as RNFL thickness). However, most studies have focused on the entire severity of glaucomatous involvement, and have reported limited diagnostic accuracy in those patients with early disease.[12, 14] Moreover, the relationship of these measurements to particular retinal regions is not clear.

Rao et al. showed that diagnostic accuracy of glaucoma using vessel density might be higher using measurements obtained from vulnerable regions such as the inferotemporal (IT) region than the global circumpapillary average.[32] In addition, Geyman et al. suggested that circumpapillary capillary density (cpCD), found by removing large vessels from the original en-face angiogram, demonstrates increased capability in detecting mild glaucoma from the control group compared to vessel density measurements without large vessel removal.[33] According to the available evidence, the diagnostic accuracy of OCT structural parameters[31] and OCTA microvascular measurements[32] are lower in eyes with milder glaucoma severity. However, an evaluation with the focus on the early stages of glaucoma has not been reported.

With this in mind, the purpose of this study was to evaluate and compare the global and regional RNFL thickness and OCTA measured microvascular parameters, to assess their diagnostic performance and to determine their association with VF in early (pre-perimetric and mild perimetric stages) POAG.

METHODS

Study Population

This was a cross-sectional study involving healthy subjects and patients with pre-perimetric and mild POAG that were recruited from the longitudinal Diagnostic Innovations in Glaucoma Study (DIGS).[34] Written informed consent was obtained from all participants. The University of California San Diego Institutional Review Board approved all protocols and methods described adhered to the tenets of the Declaration of Helsinki for research involving human subjects and the Health Insurance Portability and Accountability Act (HIPAA).

The DIGS protocol and eligibility criteria have been described in detail previously.[34] In brief, all participants underwent a comprehensive ophthalmological examination, including assessment of best corrected visual acuity, slit-lamp biomicroscopy, Goldmann applanation tonometry, gonioscopy, ultrasound pachymetry, dilated fundus examination, simultaneous stereophotography of the optic disc and visual field testing by standard automated perimetry

(Humphrey Field Analyzer; 24-2 Swedish interactive threshold algorithm; Carl Zeiss Meditec, Jena, Germany). All participants also completed Spectral-domain OCT (Avanti; Optovue, Inc.), and OCTA (Angiovue; Optovue, Inc., Fremont, CA, USA) imaging of the optic nerve head area. Perimetry and all imaging tests were conducted within a 6-month period.

Systemic measurements included systolic and diastolic blood pressure and pulse rate measured at the height of the heart with an Omron Automatic blood pressure instrument (model BP791IT; Omron Healthcare, Inc., Lake Forest, IL). Mean arterial pressure was calculated as 1/3 systolic blood pressure + 2/3 diastolic blood pressure. Mean ocular perfusion pressure was defined as the difference between 2/3 of mean arterial pressure and IOP.

Overall inclusion criteria at study entry were age of more than 18 years, open angles on gonioscopy, and best corrected visual acuity ≥ 20/40, spherical refraction within ±6.0 diopters (D), and cylinder correction within ±3.0 D. Participants included in this study were required to have good quality OCTA and Spectral-domain OCT scans and also have ≥ two reliable visual field tests. Participants with a history of intraocular surgery (except for uncomplicated cataract surgery or glaucoma surgery), coexisting retinal pathologies, non-glaucomatous optic neuropathy, uveitis, or ocular trauma were excluded from the study. Participants were also excluded if there was a diagnosis of Parkinson's disease, Alzheimer's disease, dementia, or a history of stroke. Participants with systemic hypertension and diabetes mellitus were included unless they were diagnosed with diabetic or hypertensive retinopathy. Participants who had either unreliable visual field tests or poor-quality spectral domain optic nerve head OCT or OCTA scans were also excluded.

Healthy eyes were required to have intraocular pressure (IOP) < 21 mmHg with no history of elevated IOP, normal appearing optic disc, intact neuroretinal rim and RNFL, and a minimum of 2 reliable normal visual fields, defined as a Pattern Standard Deviation (PSD) within 95% confidence limits and a Glaucoma Hemifield Test result within normal limits.[12] Pre-perimetric glaucoma eyes were defined as those having glaucomatous optic neuropathy or suspicious appearing optic discs based on stereophotograph reviewed by two experienced graders without an evidence of repeatable glaucomatous visual field damage.[8, 35, 36] A suspicious appearing optic disc was defined as a disc with observable excavation, neuroretinal rim narrowing or notching, or a localized or diffuse RNFL defect suggestive of glaucoma with stereophotographs.[34] POAG eyes were defined as those having repeatable (on at least two consecutive tests) and reliable glaucomatous visual field damage defined as a Glaucoma Hemifield Test result outside normal limits or a PSD outside 95% normal limits.[13, 37] Only early POAG eyes (24-2 mean deviation [MD] better than -6 dB)[13, 38] were included in this study. The diagnostic category for each participant was determined based on the diagnosis of worse eye.

Standard Automated Perimetry

Standard automated perimetry visual field tests were performed using Swedish Interactive Threshold Algorithm (SITA) standard 24-2 threshold test (Humphrey Field Analyzer 750 II-I, Carl Zeiss Meditec, Inc., Dublin, CA, USA). The quality of visual field tests was

reviewed by the Visual Field Assessment Center staff at the University of California San Diego. Only participants with reliable tests (33% fixation losses and false negative errors, and   33% false positive errors) were included in this study. Visual fields with the following artifacts were also excluded: evidence of rim and eyelid artifacts, inattention or fatigue effects, or visual field damage caused by a disease other than glaucoma.

For regional analyses, threshold values at each test location were used according to the Garway-Heath structure-function map.[39, 40] Total deviation in dB at each test location was converted to the linear scale of 1/Lambert (1/L) and then averaged over the entire regional test points to obtain the average total deviation in a linear scale. Regional total deviation was then converted back to the dB scale.

Optical Coherence Tomography Angiography and Spectral-Domain Optical Coherence Tomography

OCTA and Spectral-domain OCT and imaging of the nerve head (ONH) were performed by the AngioVue imaging system (Optovue, Inc., Fremont, CA, USA, Version 2017,1,0,151). Using this system, OCTA and Spectral-domain OCT images are obtained from the same scans allowing precise registration of the analyzed regions of interest. The AngioVue provides a noninvasive OCT-based method for visualizing the vascular structures of the retina. It uses split-spectrum amplitude-decorrelation angiography (SSADA) algorithm to capture the dynamic motion of red blood cells from sequential cross-sectional B-scans providing high-resolution 3D visualization of perfused retinal vasculature at various user-defined layers of the retina at the capillary level. Angiovue software automatically calculates vessel density as the proportion of measured area occupied by flowing blood vessels defined as pixels having decorrelation values above a set threshold level. As a result, thickness and vessel density measurements provided by this software come from scans with exact automated registration.

For this report, we analyzed capillary density at the radial peripapillary capillary plexus in images comprised of 304 x 304 A-scans with a 4.5 x 4.5 mm^2 field of view centered on the optic disc. The retinal layers of each scan were automatically segmented by the AngioVue software in order to visualize the radial peripapillary capillary plexus layer in a slab from internal limiting membrane to RNFL posterior boundary. Capillary density measurements were obtained after the automated removal of large vessels from the original en-face angiogram using the Angiovue software. Whole image CD (wiCD) and cpCD were included in the analysis for the assessment of the global ONH microvascular structure. WiCD measurements were calculated over the entire 4.5 x 4.5 mm^2 scan area while cpCD measurements were calculated over the region defined as a 750-μm-wide elliptical annulus extending from the optic disc boundary encircling 360-degree global area. Regional capillary density measurements were calculated over the circumpapillary area divided into six consecutive sectors (Angio software version 2017,1,0,151)[41] according to the regions defined by Garway-Heath et al.[39] The boundaries of different circumpapillary regions were as follows: N: 310°-60°, SN: 60°-100°, ST: 100°-140°, T: 140°-230°, IT: 230°-270°, IN: 270°-310°. The optic nerve cube scanning protocol was used to measure the circumpapillary

RNFL thickness of the same scan slab as OCTA scan. Global average and regional measurements corresponding to the predefined regions were used for the analysis.

Image quality review was completed on all scans according to a standard protocol established by the Imaging Data Evaluation and Analysis Reading Center. Trained graders reviewed scans and excluded poor quality images, defined as images with 1) a signal strength index (SSI) of less than 48 (1= minimum, 100 = maximum), 2) poor clarity[42] 3) residual motion artifacts visible as irregular vessel pattern or disc boundary on the en-face angiogram,[42] 4) local weak signal by artifacts such as floaters,[42] 5) RNFL segmentation errors. The location of the disc margin was reviewed for accuracy and manually adjusted if required.

Statistical Analysis

The distribution of continuous variables was assessed by inspecting histograms and using Shapiro-Wilk W test of normality. Patient and eye characteristics data were presented as mean (95% CI) for continuous variables and count (%) for categorical variables. Overall significance was determined by ANOVA (with adjusted P-values for pairwise comparisons using Bonferroni's correction) and Fisher's exact test (same for pairwise comparisons) for continuous and categorical patient level variables. Significance and estimates were derived from linear mixed models for eye level characteristics and the P-values for pairwise comparisons were adjusted using Bonferroni's correction. Mean and 95% CI for RNFL thickness and capillary density parameters were presented by each diagnostic group. P-values were presented as unadjusted (age and SSI adjusted). Significance was determined by linear mixed effects models. Linear mixed effects models were used to determine the association between global and regional RNFL thickness and capillary density measurements in each diagnostic group. The strength of association was reported as R-squared (95% CI).

In pre-perimetric and mild perimetric glaucoma eyes, RNFL thickness (μm) and capillary density (%) that are originally measured in different units were adjusted and then mapped to a relative loss scale for direct comparison of the magnitudes of loss.[43-46] RNFL thickness measurements were age adjusted. Capillary density measurements were age and SSI adjusted since a previous study showed that OCTA derived microvascular measurements are significantly affected by SSI.[47] After adjustment, Z-score normalization[48] was performed based on the distribution of each parameter of interest in the healthy eyes (n = 80) using the following formula:

$$Z - \text{score normalized loss value} = \frac{\text{adjusted target value} - \text{mean value of the healthy group}}{\text{standard deviation of the healthy group}}$$

The area under the receiver operating characteristics curve (AUROC) [and bias corrected bootstrap 95% CI] was used to determine the classification accuracy of global and regional RNFL thickness and capillary density measurements to discriminate healthy/pre-perimetric glaucoma and healthy/mild glaucoma eyes. Sensitivities at fixed levels of specificity were also reported. A pairwise bootstrap method was used to compared the global and regional RNFL thickness and capillary density accuracies to discriminate between diagnostic groups.

Linear mixed effects models were used to assess RNFL thickness-VF mean total deviation and capillary density-VF mean total deviation correlations both globally and regionally at each diagnostic group. A pairwise bootstrap method was used to assess the significance of difference in the strengths of association between RNFL thickness-VF mean total deviation and capillary density-VF mean total deviation pairs. Univariable mixed effects models were used to determine the association between SSI, demographic, and ocular parameters with VF MD. Variables with $P < 0.1$ in the univariable model were included in a final multivariable model. Statistical analyses were performed using Stata version 15.1 (StataCorp, College Station, TX), and R version 3.6.3. P values of less than 0.05 were considered statistically significant for all analyses.

RESULTS

A total of 223 patients (328 eyes), including 48 healthy subjects (80 eyes), 25 pre-perimetric glaucoma (64 eyes), and 150 mild glaucoma patients (184 eyes) were enrolled in this cross-sectional study. Glaucoma eyes had worse MD (−2.82 dB [95% CI: −3.08, −2.56]) and higher PSD (3.97 dB [95% CI: 3.64, 4.31]) comparing to healthy and pre-perimetric glaucoma eyes ($P < 0.001$ for both comparisons) while other ocular characteristics were the same among different diagnostic groups. Patient characteristics and ocular factors are summarized across different diagnostic categories in Table 1.

Comparison of RNFL thickness and capillary density among different diagnostic groups

Glaucoma eyes had lower global RNFL thickness (80.8 μm [95% CI: 78.3, 83.3]) compared to pre-perimetric glaucoma (90.1 μm [95% CI: 86.5, 93.7]) and healthy eyes (99.9 μm [95% CI: 95.6, 104.2]) ($P < 0.001$). The highest and lowest absolute regional differences between healthy and glaucoma eyes in RNFL thickness were observed in the IT (34.7 μm [95% CI: 26.7, 42.7]) and temporal (3.1 μm [95% CI: −0.2, 6.3]) regions, respectively.

Similarly, wiCD and cpCD of glaucoma eyes (42.4 % [95% CI: 41.6, 43.1]), and (43.8 % [95% CI: 43.0, 44.6], respectively) were lower than those of healthy eyes (49.0 % [95% CI: 47.8, 50.2]), and (51.1 % [95% CI: 49.7, 52.5], respectively) ($P < 0.001$ for both). The highest and lowest absolute regional differences between healthy and glaucoma eyes in capillary density were observed in the IT (11.2%, 95% CI: 8.6, 13.8) and T (4.1%, 95% CI: 2.7, 5.4) regions, respectively. Details of global and regional RNFL thickness and capillary density measurements in each diagnostic category are shown in Table 2.

RNFL thickness-capillary density relationship

Strong, and statistically significant associations were found between RNFL thickness and capillary density, globally ($R^2 = 0.571$ [95% CI: 0.510, 0.629]) and in all different regions ($P < 0.001$). The strongest regional association between RNFL thickness and capillary density was found in the IT region (R-squared = 0.542 [0.478, 0.603]). (Figure 1, Supplemental Table 1)

In healthy eyes, global RNFL thickness and capillary density were not significantly associated ($P = 0.134$), while this association was statistically significant in the N, IN, SN, T regions (all $P < 0.05$). Pre-perimetric eyes showed statistically significant associations

between RNFL thickness and capillary density, globally (R-squared = 0.390 [95% CI: 0.223, 0.556]), and in different regions (all *P* < 0.001) with the strongest regional association between RNFL thickness and capillary density was found in the IN region (R-squared = 0.466 [95% CI: 0.305, 0.618]). Glaucoma eyes showed the strongest associations between RNFL thickness and capillary density measurements compared to other diagnostic groups (*P* for global and regional associations < 0.05). In the glaucoma group, global RNFL thickness and capillary density measurements were strongly associated (R-squared = 0.548 [95% CI: 0.463, 0.628]) and the IT region had the strongest regional association (R-squared = 0.633 [95% CI: 0.561, 0.700]). (Figure 1, Supplemental Table 1)

RNFL thickness and capillary density relative loss comparison

Figure 2 shows global and regional relative loss in capillary density and RNFL thickness measurements of pre-perimetric and glaucoma eyes. In pre-perimetric glaucoma eyes, mean relative loss in capillary density was higher than that in RNFL thickness globally and in all regions except for the SN (*P* = 0.547) region (*P* < 0.05). The same comparison in glaucoma eyes showed a similar trend of greater capillary density loss than RNFL thickness loss globally and in different regions (*P* < 0.05) except for the IN (*P* = 0.475) and SN (*P* = 0.681) regions. (Supplemental Table 2)

Separate analyses revealed greater proportions of eyes with considerable microvascular loss (defined as age and SSI adjusted cpCD Z-score < −2.5 SD of the distribution of the same parameter in healthy eyes) than the proportions of eyes with considerable RNFL thickness loss at pre-perimetric glaucoma (25.0 % vs 10.9 %) and glaucoma (28.8 % vs 17.9%) stages. (Supplemental Figure 1) Moreover, greater global magnitudes of capillary density loss than RNFL thickness loss were observed in 67.2% of pre-perimetric glaucoma and 61.4% glaucoma eyes at the individual level. Pre-perimetric glaucoma and glaucoma eyes with greater capillary density than RNFL thickness loss were more likely to be of non-African American origin (OR = 2.00, *P* = 0.043), have lower cpCD (OR = 1.31 [per 1% capillary density reduction], *P* < 0.001) and have higher IOP measurements (OR = 1.07 [per 1 mmHg increase in IOP], *P* = 0.043) than those with greater RNFL thickness loss. Figure 3 shows the individual relative loss measurements in pre-perimetric glaucoma and glaucoma groups.

Performance of RNFL thickness and capillary density measurements for the detection of pre-perimetric glaucoma and glaucoma

The AUROCs for the classification accuracy of global RNFL thickness, wiCD, and cpCD to distinguish healthy from pre-perimetric glaucoma eyes were 0.716 (95% CI: 0.601, 0.819), 0.829 (95% CI: 0.736, 0.907), and 0.809 (0.712, 0.895), respectively. WiCD (AUROC = 0.829 [95% CI: 0.736, 0.907]), and cpCD (AUROC = 0.809 [95% CI: 0.712, 0.895]) were superior to RNFL thickness in the classification of healthy from pre-perimetric glaucoma eyes (*P* = 0.018, and *P* = 0.047 for the differences in AUROCs, respectively). The SN region among regional RNFL thickness measurements and the N region among regional capillary density measurements had the highest classification accuracy to distinguish healthy eyes from pre-perimetric glaucoma eyes (AUROCs of 0.787 [95% CI: 0.679, 0.870], and 0.796 [95% CI: 0.694, 0.882], respectively). For this classification, capillary density values were superior to RNFL thickness measurements in the N, ST, and T regions (*P* < 0.05).

(Table 3) Structural measurements including RNFL thickness and capillary density had a better diagnostic performance (higher AUROCs) in classifying glaucoma/healthy eyes than that of pre-perimetric glaucoma/healthy eyes. The AUROCs of this classification for global RNFL thickness, wiCD, and cpCD were 0.819 (95% CI: 0.755, 0.876), 0.876 (95% CI: 0.821, 0.918), and 0.866 (95% CI: 0.809, 0.909), respectively. The IN region for RNFL thickness measurements and the IT region for capillary density values had the highest regional classification accuracies (AUROCs of 0.815 [95% CI: 0.748, 0.872], and 0.814 [95% CI: 0.753, 0.867], respectively). Regional classification performance of RNFL thickness measurements were similar to those of capillary density values except for the N ($P = 0.007$) and T ($P < 0.001$) regions. (Table 4)

RNFL thickness-function and capillary density-function relationship

When all diagnostic groups were included, VF mean total deviation was significantly correlated with RNFL thickness and capillary density globally and in all regions ($P < 0.05$) except with RNFL thickness in the T region ($P = 0.070$). Strength of association with visual function was similar for global RNFL thickness (R-squared = 0.152 [95% CI: 0.089, 0.226]) and capillary density (R-squared = 0.160 [95% CI: 0.096, 0.235]), ($P = 0.396$). The ST and IT regions showed the highest regional strengths of association between visual function-RNFL thickness (R-squared = 0.301, 0.227; respectively) and visual function-capillary density (R-squared = 0.338, 0.246; respectively) [$P < 0.001$]. RNFL thickness and capillary density had similar strengths of association with visual function in different regions ($P > 0.05$) except in the T region ($P = 0.047$). [Figure 4, Supplemental Table 3]

In pre-perimetric glaucoma eyes, the associations between global and regional visual function-RNFL thickness were not statistically significant except for the ST region (R-squared = 0.080, $P = 0.039$). Interestingly, the association between visual function-capillary density was statistically significant in the N, IT, and ST regions ($P < 0.05$) in the same diagnostic group. Pre-perimetric glaucoma eyes had the strongest visual function-capillary density association in the ST region (R-squared = 0.161 [95% CI: 0.034, 0.341]).

Glaucoma eyes showed statistically significant associations between visual function-RNFL thickness and visual function-capillary density globally and in all regions ($P < 0.05$) except for the visual function-RNFL thickness association in the IN ($P = 0.090$) and T ($P = 0.218$) regions. There was no significant difference in the strength of global and regional associations between visual function-RNFL thickness and visual function-capillary density in glaucoma eyes. The strongest regional association between visual function-RNFL thickness and visual function-capillary density was found in the ST region (R-squared of 0.297 [0.198, 0.402], and 0.316 [0.216, 0.420], respectively). (Figure 4, Supplemental Table 3)

In the univariable analysis, age, rim area, global RNFL thickness, wiCD, cpCD, and SSI had statistically significant associations with VF MD ($P < 0.05$). Global RNFL thickness, cpCD, and SSI remained statistically significant associated with VF MD after adjusting for correlations between the independent variables in the multivariable model ($P < 0.05$). (Supplemental Table 4)

DISCUSSION

The advent of more sensitive technologies into medicine brings about a chance for earlier diagnosis and intervention with a potentially favorable disease outcome. The results of the present study support the utility of microvascular imaging using OCTA to detect glaucoma associated changes earlier in the course of disease progression, notably in the pre-perimetric stage. Our findings indicate that vascular and thickness measurements have a strong topographical association in the pre-perimetric and perimetric glaucoma stages. Similarly, relatively strong vascular-function and structure-function associations were seen globally and in different regions in mild glaucoma. VF MD remained independently associated with both vascular and thickness parameters suggesting both of these assessments for evaluating glaucoma progression earlier in the course of the disease.

Global and regional RNFL thickness thinning and retinal microvascular density dropout was associated with increasing severity of glaucoma. This is consistent with previous findings showing decreased RNFL thickness,[12, 14] and retinal microvasculature[12, 14, 33, 49] in glaucoma eyes compared to normal eyes. However, those studies (except[33]) included glaucoma eyes from the whole spectrum of disease severity, whereas only mild glaucoma eyes were included in our study. It can be inferred that the glaucomatous structural changes are evident at the early perimetric stage of the disease. More importantly, we demonstrated that OCT and OCTA instruments are sensitive enough to detect anatomical changes at the disease's pre-perimetric stage. Detecting RNFL thickness loss at the pre-perimetric stage of glaucoma, many prior studies failed to demonstrate a corresponding change in retinal microvascular assessments.[12, 14, 49] On the other hand, findings of the intact hemiretinae of glaucoma patients with single hemifield visual field defect[50] and those of the fellow eyes of glaucoma patients with unilateral visual field loss[51] suggest the presence of microvascular dropout before an identifiable visual field defect. Our results with a special focus on early glaucoma spectrum confirm a measurable reduction in retinal microvasculature before the development of an identifiable visual field defect.

Strong regional correlations were observed between retinal thickness and microvasculature at the pre-perimetric and early perimetric stages of glaucoma, indicating that topographical changes in thickness and microvasculature are associated with each other. However, the proportions of eyes with considerable microvasculature loss was higher than those of eyes with considerable RNFL thickness loss at the pre-perimetric and perimetric glaucoma stages. In addition, a separate analysis at the individual level showed a greater loss in microvasculature than RNFL thickness in 67% of the pre-perimetric and 61% of the perimetric glaucoma eyes. This finding merits specific attention at the pre-perimetric stage showing the potential for using microvascular measurements alongside RNFL thickness assessments to detect the disease at a stage where functional tests are not sensitive enough. Moreover, a sub analysis at the level of pre-perimetric glaucoma and glaucoma eyes suggested that eyes with greater microvascular loss might have different characteristics in terms of ethnicity, IOP and cpCD comparing to those with greater RNFL thickness loss. Recently, studies on early glaucoma patients have identified discrepancies at the individual level in terms of relative magnitudes of macular vessel density versus ganglion cell thickness loss suggesting different subtypes of early glaucomatous damage

associated with greater ganglion cell or vascular density reduction in the macular area.[44, 45] Moreover, Hirasawa et al.[45] have suggested that these different subtypes are associated with different demographic and ocular characteristics in terms of gender and RNFL thickness. Considering that individual characteristics are associated with different magnitudes of microvascular or thickness loss in glaucoma, evaluating microvasculature alongside thickness is recommended especially in a subset of patients with a higher likelihood of greater microvascular than RNFL thickness loss at an earlier stage.

Retinal capillary blood flow is decreased even before the development of visual field defects in POAG.[52] We demonstrated that retinal microvascular assessment has better diagnostic accuracy than RNFL thickness measurement in discriminating pre-perimetric glaucoma, and glaucoma eyes from normal eyes. Previous studies on VD and RNFL thickness to discriminate pre-perimetric glaucoma from normal eyes yielded similar performance between these measurements.[12, 14, 53] They reported diagnostic performance of RNFL thickness and VD in pre-perimetric glaucoma eyes to be 0.65, and 70;[12] 0.70, and 0.60;[49] and 0.65, and 0.51;[14] without statistically significant differences. However, Yarmohammadi et al.,[12] and Triolo et al.[14] used the overall vessel density measurements in their studies without removing large vessels' effects. It is demonstrated that capillary density, which is provided by subtracting large vessels from the original angiogram, shows high intrasession and intersession reproducibility and provides a higher diagnostic accuracy compared to VD in POAG.[54] In this respect, the mean intrasession coefficients of variation (CVs) for the wiCD and cpCD were reported to be 1.0 ± 0.8 and 1.3 ± 0.9 in healthy eyes and 1.5 ± 1.0 and 1.8 ± 1.2 in POAG eyes, respectively. The mean inter-session CVs for the wiCD and cpCD were 1.9 ± 0.7 and 1.2 ± 0.5 in healthy eyes, respectively.[54] Improvements in imaging techniques and the software for microvascular calculation might have led to increased sensitivity for detecting subtle changes happening earlier in glaucoma progression that has not been possible before.

Regional correlation of visual function to its corresponding structural measurements is suggested to be the best way of evaluating structure-function relationship in glaucoma.[55] Previous studies on the association of visual function and vascular parameters mostly focused on global measurements of OCTA and VF testing machines that are averaged over a large scale.[12, 13, 56] This approach is liable to miss the potential structure-function correlations in smaller anatomical regions that would probably be seen earlier in the course of glaucoma progression. We found significant vascular-function and thickness-function relationships in all anatomical regions in mild glaucoma (except for thickness-function relationship in IN and T regions; P-values of 0.090 and 0.218, respectively). Moreover, the strength of association between vascular-function and the thickness-function relationship was similar in different anatomical regions in the same diagnostic group. Prior studies evaluating the regional structure-function relationship in glaucoma using OCT and OCTA found ST and IT sectors as the regions with the highest structure-function association.[4, 57] These regions showed the strongest structure-function association in our study, confirming previous reports on the vulnerability of these areas to early glaucomatous damage.[57, 58] Rao and colleagues evaluated glaucoma patients with all classes of disease severity using OCT and found the highest association in the IT sector ($r^2 = 0.26$) followed by the ST sector ($r^2 = 0.22$) with a slight difference.[4] In another study by Shin et al. using OCTA, the IT sector

showed the highest association (r = 0.650) followed by the ST sector (r = 0.579) among glaucoma patients with all classes of disease severity. However, the ST sector showed a slightly higher structure-function association compared to the IT sector when considering only mild glaucoma subjects (r = 0.442 and 0.426, respectively).[57] Notably, both of these studies used a prior definition to demarcate the regional boundaries as 45 degrees apart. Recently, this definition has been slightly modified by the commercial Angiovue software (as used in this study) in order to enhance the structure-function association. Our findings are similar to those of prior studies in terms of ST and IT regions as the areas with the highest structure-function relationship, and the ST region had a higher structure-function association than the IT sector. At least in part, the inclusion of early glaucoma patients and slight modification of the regional boundaries might account for the observed findings. Moreover, most of our study population were of European or African descent while Shin's study was conducted on an ethnically homogenous Korean population.

Interestingly, N, IT and ST regions showed significant vascular-function associations in the pre-perimetric glaucoma group with a fair degree of strength of association in the ST region. These regions are the ones that are most vulnerable to glaucomatous damage at an early stage.[59] Stronger associations for vascular-thickness than those for structure-function relationship in the present study is consistent with the findings of a prior study.[13] Regional microvascular dropout is evident in the early stage of glaucoma before visual field damages are detectable.

Visual field loss was correlated with both vessel density and RNFL thickness in multivariable model. Our results are in agreement with those of prior studies[13, 57], and suggest that retinal vascular and thickness evaluations can provide independent information about the functional status earlier in the disease course.

To date, this is the largest study focusing on structural alterations in the early spectrum of POAG. Automatic translations of enface-angiogram and thickness maps, removal of large vessels and adjustments for the effects of SSI on vessel density measurements contrast our findings to those previously found by similar studies. However, our study is bound by the limitations arising from the nature of cross-sectional designs. Accordingly, longitudinal investigations are needed to elucidate the temporality of thickness and vascular damage in different stages of glaucoma with the hope of finding a plausible mechanism explaining the nature of glaucoma progression. Another limitation is the possible effect of treatment, including antiglaucoma eye drops that might have influenced our vascular assessments and the disease's natural course. Finally, different OCTA devices use different algorithms for assessment of vessel density and measurements obtained by Optovue might not be generalizable to other devices.

In conclusion, capillary density and RNFL thickness were decreased in pre-perimetric and mild glaucoma eyes compared to healthy eyes. Microvascular dropout was higher than thickness loss in patients with similar functional status and capillary density had a greater diagnostic accuracy than RNFL thickness in detecting pre-perimetric and mild glaucoma globally as wells as in some regions. Greater capillary density compared to thickness loss was found in about two-thirds of pre-perimetric and mild glaucoma eyes and was associated

with individual characteristics. Vascular-function associations were found in the vulnerable regions of pre-perimetric and all regions of mild glaucoma. Thickness and microvascular assessments are complementary and yield valuable information for the detection of early damages seen in POAG.

Supplementary Material

Refer to Web version on PubMed Central for supplementary material.

Acknowledgement:

Abbreviations and Acronyms:

AL	axial length
AUROC	area under the receiver operating characteristics curve
CCT	central corneal thickness
cpCD	circumpapillary capillary density
D	Diopter
DIGS	diagnostic innovations in glaucoma study
HIPAA	health insurance portability and accountability act
IN	inferonasal
IOP	intraocular pressure
IT	inferotemporal
L	Lambert
MAP	mean arterial pressure
MD	mean deviation
MOPP	mean ocular perfusion pressure
N	nasal
OCTA	optical coherence tomography angiography
ONH	optic nerve head
POAG	primary open angle glaucoma
PSD	pattern standard deviation

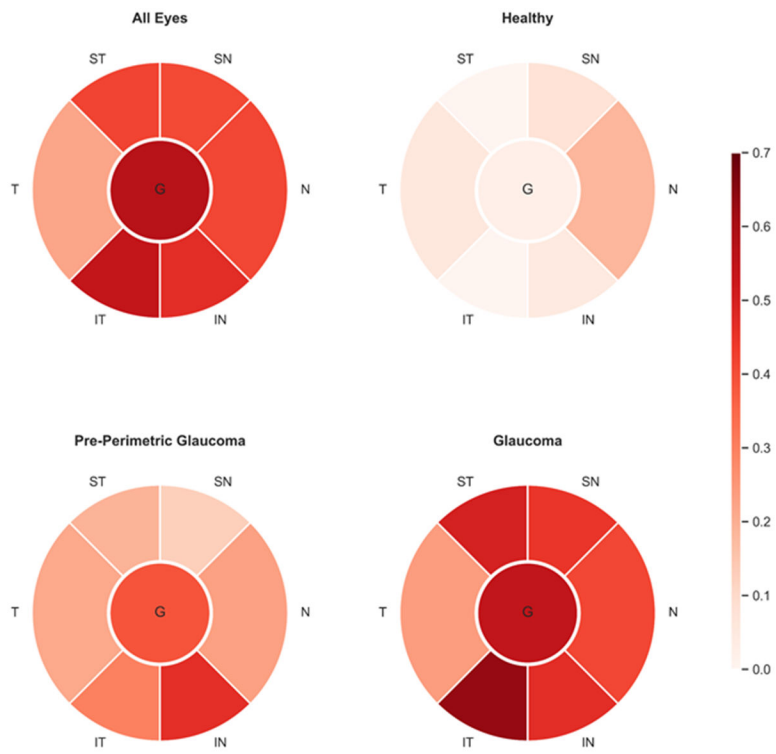| **RNFL** | retinal nerve fiber layer |
SD	standard deviation
SITA	Swedish interactive threshold algorithm
SN	superonasal
SSADA	split-spectrum amplitude-decorrelation angiography
SSI	signal strength index
ST	superotemporal
T	temporal
VF	visual field
OCT	optical coherence tomography
wiCD	Whole image capillary density

References

1. Weinreb RN, Aung T, Medeiros FAJJ. The pathophysiology and treatment of glaucoma: a review. 2014;311:1901–1911.

2. Weinreb RN, Leung CKS, Crowston JG, et al. Primary open-angle glaucoma. Nature Reviews Disease Primers 2016;2:16067.

3. Leske MC, Heijl A, Hussein M, et al. Factors for Glaucoma Progression and the Effect of Treatment: The Early Manifest Glaucoma Trial. Archives of Ophthalmology 2003;121:48–56. [PubMed: 12523884]

4. Rao HL, Zangwill LM, Weinreb RN, Leite MT, Sample PA, Medeiros FA. Structure-Function Relationship in Glaucoma Using Spectral-Domain Optical Coherence Tomography. Archives of Ophthalmology 2011;129:864–871. [PubMed: 21746976]

5. Medeiros FA, Zangwill LM, Bowd C, Mansouri K, Weinreb RN. The Structure and Function Relationship in Glaucoma: Implications for Detection of Progression and Measurement of Rates of Change. Investigative Ophthalmology & Visual Science 2012;53:6939–6946. [PubMed: 22893677]

6. Greenfield DS, Weinreb RN. Role of Optic Nerve Imaging in Glaucoma Clinical Practice and Clinical Trials. American Journal of Ophthalmology 2008;145:598–603.e1. [PubMed: 18295183]

7. Sakata LM, DeLeon-Ortega J, Sakata V, Girkin CA. Optical coherence tomography of the retina and optic nerve – a review. 2009;37:90–99.

8. Aydoan T, Akçay B S, Karde E, Ergin AJIjoo. Evaluation of spectral domain optical coherence tomography parameters in ocular hypertension, preperimetric, and early glaucoma. 2017;65:1143.

9. Holló GJEjoo. Vessel density calculated from OCT angiography in 3 peripapillary sectors in normal, ocular hypertensive, and glaucoma eyes. 2016;26:e42–e45.

10. Flammer J, Orgül S, Costa VP, et al. The impact of ocular blood flow in glaucoma. 2002;21:359–393.

11. Grieshaber MC, Mozaffarieh M, Flammer JJSoo. What is the link between vascular dysregulation and glaucoma? 2007;52:S144–S154.

12. Yarmohammadi A, Zangwill LM, Diniz-Filho A, et al. Optical Coherence Tomography Angiography Vessel Density in Healthy, Glaucoma Suspect, and Glaucoma Eyes. Investigative Ophthalmology & Visual Science 2016;57:OCT451–OCT459. [PubMed: 27409505]

13. Yarmohammadi A, Zangwill LM, Diniz-Filho A, et al. Relationship between Optical Coherence Tomography Angiography Vessel Density and Severity of Visual Field Loss in Glaucoma. Ophthalmology 2016;123:2498–2508. [PubMed: 27726964]

14. Triolo G, Rabiolo A, Shemonski ND, et al. Optical Coherence Tomography Angiography Macular and Peripapillary Vessel Perfusion Density in Healthy Subjects, Glaucoma Suspects, and Glaucoma Patients. Investigative Ophthalmology & Visual Science 2017;58:5713–5722. [PubMed: 29114838]

15. Garas A, Vargha P, Hollo GJE. Diagnostic accuracy of nerve fibre layer, macular thickness and optic disc measurements made with the RTVue-100 optical coherence tomograph to detect glaucoma. 2011;25:57–65.

16. Schulze A, Lamparter J, Pfeiffer N, et al. Diagnostic ability of retinal ganglion cell complex, retinal nerve fiber layer, and optic nerve head measurements by Fourier-domain optical coherence tomography. 2011;249:1039–1045.

17. Bertuzzi F, Benatti E, Esempio G, Rulli E, Miglior SJJoG. Evaluation of retinal nerve fiber layer thickness measurements for glaucoma detection: GDx ECC versus spectral-domain OCT. 2014;23:232–239.

18. Begum VU, Addepalli UK, Yadav RK, et al. Ganglion cell-inner plexiform layer thickness of high definition optical coherence tomography in perimetric and preperimetric glaucoma. 2014;55:4768–4775.

19. Lisboa R, Paranhos A, Weinreb RN, et al. Comparison of different spectral domain OCT scanning protocols for diagnosing preperimetric glaucoma. 2013;54:3417–3425.

20. Sung KR, Na JH, Lee YJJog. Glaucoma diagnostic capabilities of optic nerve head parameters as determined by Cirrus HD optical coherence tomography. 2012;21:498–504.

21. Rao HL, Kumbar T, Addepalli UK, et al. Effect of spectrum bias on the diagnostic accuracy of spectral-domain optical coherence tomography in glaucoma. 2012;53:1058–1065.

22. Rao HL, Zangwill LM, Weinreb RN, Sample PA, Alencar LM, Medeiros FAJO. Comparison of different spectral domain optical coherence tomography scanning areas for glaucoma diagnosis. 2010;117:1692–1699. e1.

23. Nakatani Y, Higashide T, Ohkubo S, Takeda H, Sugiyama KJJog. Evaluation of macular thickness and peripapillary retinal nerve fiber layer thickness for detection of early glaucoma using spectral domain optical coherence tomography. 2011;20:252–259.

24. Firat PG, Doganay S, Demirel EE, Colak CJGsAfC, Ophthalmology E. Comparison of ganglion cell and retinal nerve fiber layer thickness in primary open-angle glaucoma and normal tension glaucoma with spectral-domain OCT. 2013;251:831–838.

25. Arintawati P, Sone T, Akita T, Tanaka J, Kiuchi YJJog. The applicability of ganglion cell complex parameters determined from SD-OCT images to detect glaucomatous eyes. 2013;22:713–718.

26. Rolle T, Briamonte C, Curto D, Grignolo FMJCO. Ganglion cell complex and retinal nerve fiber layer measured by fourier-domain optical coherence tomography for early detection of structural damage in patients with preperimetric glaucoma. 2011;5:961.

27. Rao H, Babu J, Addepalli U, Senthil S, Garudadri CJE. Retinal nerve fiber layer and macular inner retina measurements by spectral domain optical coherence tomograph in Indian eyes with early glaucoma. 2012;26:133–139.

28. Barua N, Sitaraman C, Goel S, Chakraborti C, Mukherjee S, Parashar HJIjoo. Comparison of diagnostic capability of macular ganglion cell complex and retinal nerve fiber layer among primary open angle glaucoma, ocular hypertension, and normal population using Fourier-domain optical coherence tomography and determining their functional correlation in Indian population. 2016;64:296.

29. Moreno PA, Konno B, Lima VC, et al. Spectral-domain optical coherence tomography for early glaucoma assessment: analysis of macular ganglion cell complex versus peripapillary retinal nerve fiber layer. 2011;46:543–547.

30. Kim YJ, Kang MH, Cho HY, Lim HW, Seong MJJjoo. Comparative study of macular ganglion cell complex thickness measured by spectral-domain optical coherence tomography in healthy eyes, eyes with preperimetric glaucoma, and eyes with early glaucoma. 2014;58:244–251.

31. Aydogan T, Akçay B S, Karde E, Ergin A. Evaluation of spectral domain optical coherence tomography parameters in ocular hypertension, preperimetric, and early glaucoma. Indian J Ophthalmol 2017;65:1143–1150. [PubMed: 29133640]

32. Rao HL, Pradhan ZS, Weinreb RN, et al. Regional Comparisons of Optical Coherence Tomography Angiography Vessel Density in Primary Open-Angle Glaucoma. American Journal of Ophthalmology 2016;171:75–83. [PubMed: 27590118]

33. Geyman LS, Garg RA, Suwan Y, et al. Peripapillary perfused capillary density in primary open-angle glaucoma across disease stage: an optical coherence tomography angiography study. British Journal of Ophthalmology 2017;101:1261. [PubMed: 28148529]

34. Sample PA, Girkin CA, Zangwill LM, et al. The african descent and glaucoma evaluation study (ADAGES): Design and baseline data. 2009;127:1136–1145.

35. Cennamo G, Montorio D, Velotti N, et al. Optical coherence tomography angiography in pre-perimetric open-angle glaucoma. 2017;255:1787–1793.

36. Cvenkel B, Sustar M, Perovšek DJDO. Ganglion cell loss in early glaucoma, as assessed by photopic negative response, pattern electroretinogram, and spectral-domain optical coherence tomography. 2017;135:17–28.

37. Yarmohammadi A, Zangwill LM, Manalastas PIC, et al. Peripapillary and macular vessel density in patients with primary open-angle glaucoma and unilateral visual field loss. 2018;125:578–587.

38. Hodapp E, Parrish R, Anderson DJP. Clinical Decisions in Glaucoma St Louis, Mo: Mosby; 1993.

39. Garway-Heath DF, Poinoosawmy D, Fitzke FW, Hitchings RAJO. Mapping the visual field to the optic disc in normal tension glaucoma eyes. 2000;107:1809–1815.

40. Kumar RS, Anegondi N, Chandapura RS, et al. Discriminant function of optical coherence tomography angiography to determine disease severity in glaucoma. 2016;57:6079–6088.

41. Kumar RS, Anegondi N, Chandapura RS, et al. Discriminant Function of Optical Coherence Tomography Angiography to Determine Disease Severity in Glaucoma. Investigative Ophthalmology & Visual Science 2016;57:6079–6088. [PubMed: 27820876]

42. Kamalipour A, Moghimi S, Hou H, et al. OCT Angiography Artifacts in Glaucoma. Ophthalmology 2021.

43. Hou H, Moghimi S, Proudfoot JA, et al. Ganglion Cell Complex Thickness and Macular Vessel Density Loss in Primary Open-Angle Glaucoma. Ophthalmology 2020;127:1043–1052. [PubMed: 32085875]

44. Hou H, Moghimi S, Zangwill LM, et al. Macula Vessel Density and Thickness in Early Primary Open-Angle Glaucoma. American journal of ophthalmology 2019;199:120–132. [PubMed: 30496723]

45. Hirasawa K, Smith CA, West ME, et al. Discrepancy in Loss of Macular Perfusion Density and Ganglion Cell Layer Thickness in Early Glaucoma. American Journal of Ophthalmology 2021;221:39–47. [PubMed: 32828878]

46. Hou H, Moghimi S, Kamalipour A, et al. Macular Thickness and Microvasculature Loss in Glaucoma Suspect Eyes. Ophthalmology Glaucoma 2021.

47. Yu JJ, Camino A, Liu L, et al. Signal Strength Reduction Effects in OCT Angiography. Ophthalmology Retina 2019;3:835–842. [PubMed: 31257069]

48. Rosner B Fundamentals of biostatistics: Cengage learning, 2015.

49. Chen C-L, Zhang A, Bojikian KD, et al. Peripapillary Retinal Nerve Fiber Layer Vascular Microcirculation in Glaucoma Using Optical Coherence Tomography-Based Microangiography. Investigative ophthalmology & visual science 2016;57:OCT475–OCT485. [PubMed: 27442341]

50. Yarmohammadi A, Zangwill LM, Diniz-Filho A, et al. Peripapillary and Macular Vessel Density in Patients with Glaucoma and Single-Hemifield Visual Field Defect. Ophthalmology 2017;124:709–719. [PubMed: 28196732]

51. Yarmohammadi A, Zangwill LM, Manalastas PIC, et al. Peripapillary and Macular Vessel Density in Patients with Primary Open-Angle Glaucoma and Unilateral Visual Field Loss. Ophthalmology 2018;125:578–587. [PubMed: 29174012]

52. Michelson G, Langhans MJ, Harazny J, Dichtl A. Visual field defect and perfusion of the juxtapapillary retina and the neuroretinal rim area in primary open-angle glaucoma. Graefe's Archive for Clinical and Experimental Ophthalmology 1998;236:80–85.

53. Chen C-L, Zhang A, Bojikian KD, et al. Peripapillary Retinal Nerve Fiber Layer Vascular Microcirculation in Glaucoma Using Optical Coherence Tomography–Based Microangiography. Investigative Ophthalmology & Visual Science 2016;57:OCT475–OCT485. [PubMed: 27442341]

54. Geyman LS, Garg RA, Suwan Y, et al. Peripapillary perfused capillary density in primary open-angle glaucoma across disease stage: an optical coherence tomography angiography study. 2017;101:1261–1268.

55. Hood DC, Anderson SC, Wall M, Kardon RH. Structure versus Function in Glaucoma: An Application of a Linear Model. Investigative Ophthalmology & Visual Science 2007;48:3662–3668. [PubMed: 17652736]

56. Akagi T, Iida Y, Nakanishi H, et al. Microvascular Density in Glaucomatous Eyes With Hemifield Visual Field Defects: An Optical Coherence Tomography Angiography Study. American Journal of Ophthalmology 2016;168:237–249. [PubMed: 27296492]

57. Shin JW, Lee J, Kwon J, Choi J, Kook MSJBJoO. Regional vascular density–visual field sensitivity relationship in glaucoma according to disease severity. 2017;101:1666–1672.

58. Quigley HA, Addicks EM. Regional Differences in the Structure of the Lamina Cribrosa and Their Relation to Glaucomatous Optic Nerve Damage. Archives of Ophthalmology 1981;99:137–143. [PubMed: 7458737]

59. Quigley HA, Addicks EMJAoo. Regional differences in the structure of the lamina cribrosa and their relation to glaucomatous optic nerve damage. 1981;99:137–143.

Figure 1.
Global and Regional Retinal Nerve Fiber Layer Thickness and Capillary Density Associations in Each Diagnostic Group. The values of R-squared are shown in color coded format.
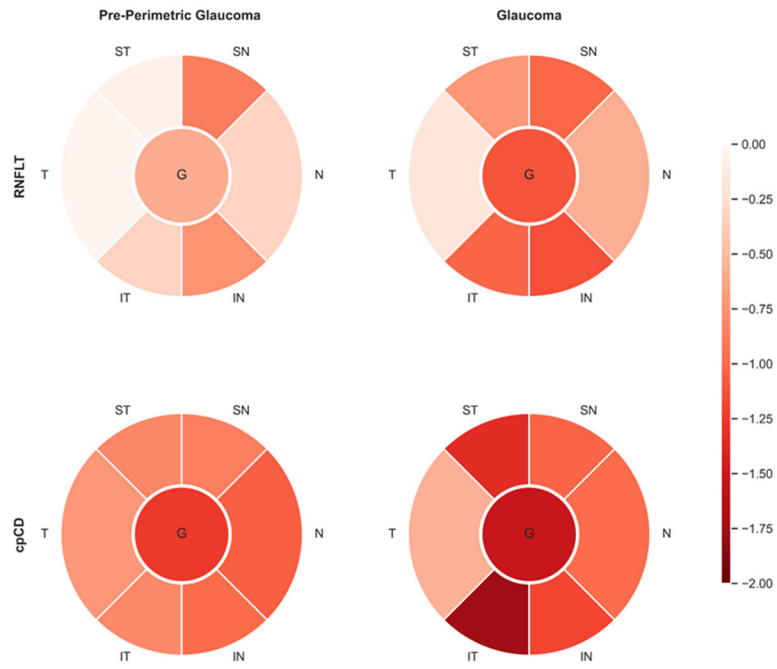
Figure 2.
Global and Regional Retinal Nerve Fiber Layer and Capillary Density Relative Loss in Pre-perimetric and Mild Perimetric Primary Open Angle Glaucoma
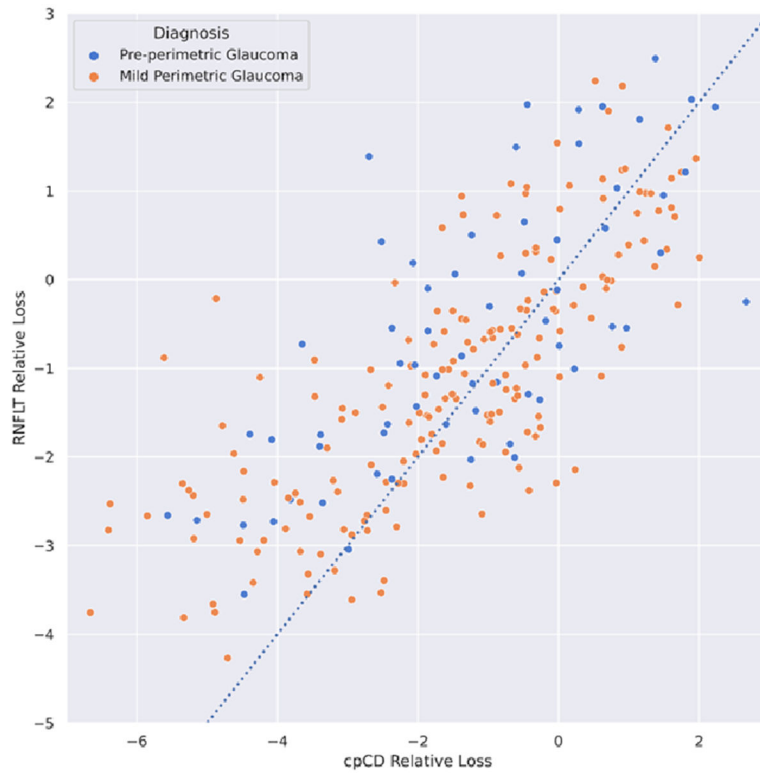
Figure 3.
Two-dimensional representation of relative global RNFL thickness (RNFLT) loss and relative circumpapillary capillary density (cpCD) loss for pre-perimetric glaucoma (blue) and mild perimetric glaucoma (orange) eyes. Points above the dashed line have higher relative loss values for circumpapillary capillary density compared to global RNFL thickness while those below the line show greater relative RNFL thickness loss.
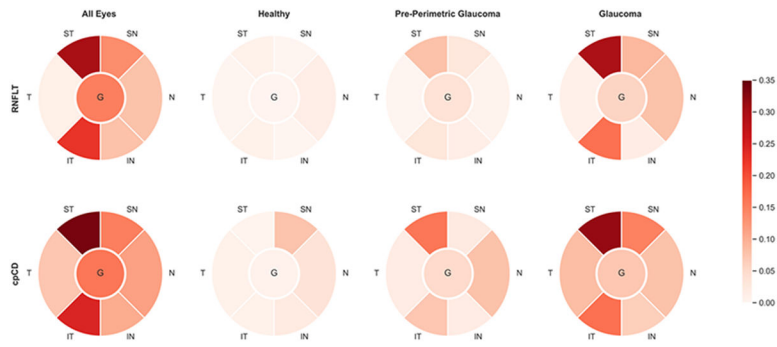
Figure 4.
Global and Regional Retinal Nerve Fiber Layer Thickness-Total Deviation and circumpapillary Capillary Density-Total Deviation Associations in Each Diagnostic Group. The values of R-squared are shown in color coded format.

Table 1.

Patient and Eye Characteristics

	Diagnosis				Pairwise Comparisons		
	A. Healthy (N = 48, Eyes = 80)	**B. Pre-Perimetric Glaucoma (N = 25, Eyes = 64)**	**C. Glaucoma (N = 150, Eyes = 184)**	**Overall P**	**A vs. B**	**A vs. C**	**B vs. C**
Patient Characteristics							
Age	62.3 (59.0, 65.6)	68.8 (63.9, 73.8)	74.0 (72.3, 75.7)	**< 0.001**	**0.050**	**< 0.001**	0.107
Race							
African American	13 (27.1%)	3 (12.0%)	42 (28.0%)				
Non-African American	35 (72.9%)	22 (88.0%)	108 (72.0%)	0.245	0.232	> 0.99	0.136
Sex							
Female	37 (77.1%)	19 (76.0%)	79 (52.7%)				
Male	11 (22.9%)	6 (24.0%)	71 (47.3%)	**0.003**	> 0.99	**0.004**	**0.032**
Hypertension							
No	28 (58.3%)	10 (40.0%)	54 (36.0%)				
Yes	20 (41.7%)	15 (60.0%)	96 (64.0%)	**0.024**	0.149	**0.007**	0.823
Diabetes							
No	44 (91.7%)	21 (84.0%)	123 (82.0%)				
Yes	4 (8.3%)	4 (16.0%)	27 (18.0%)	0.294	0.433	0.169	> 0.99
Systolic blood pressure							
	128.6 (123.4, 133.8)	131.2 (123.7, 138.7)	128.3 (125.1, 131.6)	0.830	> 0.99	> 0.99	> 0.99
Diastolic blood pressure							
	81.8 (78.8, 84.8)	83.4 (79.0, 87.8)	78.5 (76.6, 80.4)	0.090	> 0.99	0.369	0.202
MAP							
	97.4 (94.1, 100.7)	99.3 (94.2, 104.4)	95.1 (92.9, 97.2)	0.306	> 0.99	> 0.99	0.492
Eye Characteristics							
MD							
	0.12 (−0.30, 0.53)	−0.40 (−0.84, 0.03)	−2.82 (−3.08, −2.56)	**< 0.001**	0.177	**< 0.001**	**< 0.001**
PSD							
	1.61 (1.52, 1.71)	1.93 (1.74, 2.12)	3.97 (3.64, 4.31)	**< 0.001**	0.863	**< 0.001**	**< 0.001**
IOP							
	14.6 (13.5, 15.7)	16.3 (15.2, 17.4)	15.1 (14.4, 15.8)	0.062	0.063	0.932	0.088
MOPP							
	55.3 (52.7, 57.8)	53.2 (51.2, 55.3)	53.7 (52.2, 55.1)	0.463	0.440	0.564	> 0.99
CCT							
	549.5 (538.4, 560.6)	540.6 (533.4, 547.8)	540.0 (534.0, 546.0)	0.330	0.370	0.273	> 0.99
Spherical equivalent of refraction							
	−0.41 (−0.88, 0.05)	−0.52 (−0.90, −0.15)	−0.40 (−0.67, −0.14)	0.818	> 0.99	> 0.99	> 0.99
AL							
	23.7 (23.4, 24.0)	24.0 (23.9, 24.2)	24.0 (23.9, 24.2)	0.142	0.102	0.102	> 0.99

MAP: mean arterial pressure; MD: mean deviation; IOP: intraocular pressure; MOPP: mean ocular perfusion pressure; CCT: central corneal thickness; AL: axial length.

Data is presented as mean (95% CI) for continuous variables and count (%) for categorical variables. Overall significance is determined by ANOVA (with adjusted P-values for pairwise comparisons using Bonferroni's correction) and Fisher's exact test (same for pairwise comparisons) for continuous and categorical patient level variables. Significance and estimates are derived from linear mixed models for eye level characteristics and the P-values for pairwise comparisons were adjusted using Bonferroni's correction. Bolded *P* indicate statistical significance defined as *P* < 0.05.

Table 2.

Mean and 95% CI for OCT and OCTA parameters by diagnosis

	Diagnosis				Pairwise Comparisons		
	A. Healthy (N = 48, Eyes = 80)	B. Pre-Perimetric Glaucoma (N = 33, Eyes = 64)	C. Glaucoma (N = 142, Eyes = 184)	Overall P	A vs. B	A vs. C	B vs. C
Disc Area	1.91 (1.80, 2.02)	2.04 (1.95, 2.13)	1.91 (1.85, 1.98)	**0.012 (0.011)**	0.112 (0.055)	> 0.99 (> 0.99)	**0.008 (0.011)**
Overall image quality	7.5 (7.2, 7.8)	7.5 (7.2, 7.8)	7.1 (7.0, 7.3)	**0.022** (0.241)	> 0.99 (0.537)	0.051 (> 0.99)	0.064 (0.187)
SSI	6.9 (6.7, 7.1)	6.4 (6.1, 6.6)	6.2 (6.0, 6.3)	**< 0.001 (0.010)**	**0.003** (0.113)	**< 0.001 (0.005)**	0.298 (0.686)
Thickness							
Global	99.9 (95.6, 104.2)	90.1 (86.5, 93.7)	80.8 (78.3, 83.3)	**< 0.001 (< 0.001)**	**0.001 (0.032)**	**< 0.001 (< 0.001)**	**< 0.001 (< 0.001)**
N	87.0 (82.6, 91.4)	79.4 (75.4, 83.4)	73.8 (71.2, 76.4)	**< 0.001 (< 0.001)**	**0.024** (0.250)	**< 0.001 (0.001)**	**0.022** (0.051)
IN	135.2 (127.3, 143.1)	114.0 (107.4, 120.6)	100.5 (96.0, 105.0)	**< 0.001 (< 0.001)**	**< 0.001 (0.001)**	**< 0.001 (< 0.001)**	**< 0.001 (< 0.001)**
IT	129.1 (120.9, 137.4)	115.0 (107.7, 122.2)	94.2 (89.4, 99.0)	**< 0.001 (< 0.001)**	**0.022** (0.170)	**< 0.001 (< 0.001)**	**< 0.001 (< 0.001)**
ST	113.3 (106.8, 119.7)	105.9 (99.9, 111.8)	90.4 (86.6, 94.2)	**< 0.001 (< 0.001)**	0.192 (0.740)	**< 0.001 (< 0.001)**	**< 0.001 (< 0.001)**
SN	124.8 (118.0, 131.5)	103.5 (97.7, 109.2)	95.3 (91.4, 99.2)	**< 0.001 (< 0.001)**	**< 0.001 (< 0.001)**	**< 0.001 (< 0.001)**	**0.015 (0.023)**
T	64.6 (61.2, 68.0)	64.4 (61.6, 67.2)	61.3 (59.4, 63.3)	**0.050** (0.126)	> 0.99 (> 0.99)	0.199 (0.594)	0.075 (0.108)
Capillary Density							
wiCD	49.0 (47.8, 50.2)	43.9 (42.8, 45.0)	42.4 (41.6, 43.1)	**< 0.001 (< 0.001)**	**< 0.001 (< 0.001)**	**< 0.001 (< 0.001)**	**0.027** (0.135)
cpCD	51.1 (49.7, 52.5)	45.7 (44.4, 47.0)	43.8 (43.0, 44.6)	**< 0.001 (< 0.001)**	**< 0.001 (< 0.001)**	**< 0.001 (< 0.001)**	**0.014** (0.063)
N	47.9 (46.3, 49.6)	41.7 (40.1, 43.2)	40.6 (39.7, 41.6)	**< 0.001 (< 0.001)**	**< 0.001 (< 0.001)**	**< 0.001 (< 0.001)**	0.443 (> 0.99)
IN	48.9 (46.9, 50.8)	42.5 (40.6, 44.4)	40.6 (39.5, 41.8)	**< 0.001 (< 0.001)**	**< 0.001 (< 0.001)**	**< 0.001 (< 0.001)**	0.158 (0.234)
IT	56.6 (54.2, 59.0)	51.3 (48.9, 53.7)	45.3 (43.9, 46.8)	**< 0.001 (< 0.001)**	**0.004 (0.021)**	**< 0.001 (< 0.001)**	**< 0.001 (< 0.001)**
ST	53.5 (51.5, 55.5)	47.9 (45.8, 50.0)	44.1 (42.8, 45.4)	**< 0.001 (< 0.001)**	**< 0.001 (0.003)**	**< 0.001 (< 0.001)**	**0.002 (0.007)**
SN	47.7 (45.9, 49.5)	42.0 (40.3, 43.8)	40.5 (39.4, 41.6)	**< 0.001 (< 0.001)**	**< 0.001 (0.001)**	**< 0.001 (< 0.001)**	0.263 (0.547)
T	54.2 (52.8, 55.6)	50.1 (48.8, 51.4)	50.0 (49.1, 50.8)	**< 0.001 (0.004)**	**< 0.001 (0.005)**	**< 0.001 (0.003)**	> 0.99 (> 0.99)

OCT: optical coherence tomography; OCTA: optical coherence tomography angiography; SSI: signal strength index; N: nasal; IN: inferonasal; IT: inferotemporal; ST: superotemporal; SN: superonasal; T: temporal; wiCD: whole image capillary density; cpCD: circumpapillary capillary density.

P is presented as unadjusted (age and SSI adjusted). Disc area, overall image quality, and SSI are only age adjusted. Significance is determined using linear mixed effects models and *P* values for the pairwise comparisons were adjusted using Bonferroni's correction. Bolded *P* indicate statistical significance defined as *P* < 0.05.

Table 3.

Global and Regional Predictive Performance Metrics for the Differentiation of Pre-Perimetric Glaucoma from Healthy Eyes

	AUROC (95% CI)	Sensitivity At				P †
		80% Specificity	85% Specificity	90% Specificity	95% Specificity	
Thickness						
Global	0.72 (0.60, 0.82)	0.62	0.58	0.47	0.33	
N	0.68 (0.57, 0.78)	0.45	0.41	0.38	0.23	
IN	0.76 (0.66, 0.86)	0.66	0.52	0.48	0.31	
IT	0.66 (0.56, 0.77)	0.48	0.38	0.36	0.30	
ST	0.59 (0.47, 0.71)	0.42	0.38	0.33	0.12	
SN	0.79 (0.68, 0.87)	0.70	0.62	0.53	0.22	
T	0.53 (0.45, 0.61)	0.30	0.22	0.17	0.16	
Capillary Density						
wiCD	0.83 (0.74, 0.91)	0.69	0.67	0.64	0.56	**0.018**
cpCD	0.81 (0.71, 0.90)	0.70	0.66	0.62	0.58	**0.047**
N	0.80 (0.69, 0.88)	0.69	0.62	0.61	0.53	**0.016**
IN	0.77 (0.68, 0.86)	0.64	0.50	0.47	0.39	0.779
IT	0.74 (0.65, 0.83)	0.58	0.48	0.39	0.38	0.196
ST	0.73 (0.64, 0.83)	0.61	0.50	0.47	0.41	**0.013**
SN	0.72 (0.62, 0.82)	0.55	0.50	0.48	0.42	0.176
T	0.71 (0.61, 0.81)	0.53	0.48	0.38	0.30	**0.008**

AUROC: area under the receiver operating characteristic curve; N: nasal; IN: inferonasal; IT: inferotemporal; ST: superotemporal; SN: superonasal; T: temporal; wiCD: whole image capillary density; cpCD: circumpapillary capillary density.

Metrics are shown as AUROCs with bias corrected 95% confidence intervals (CI) and sensitivities at fixed specificities (Spec.) for each classifier. Significance was determined using a paired bootstrap test.

†P for the difference between AUROCs of retinal nerve fiber layer and capillary density.

Bolded P indicates statistically significant difference defined as P < 0.05.

Table 4.

Global and Regional Predictive Performance Metrics for the Differentiation of Glaucoma from Healthy Eyes

		Sensitivity At				
	AUROC (95% CI)	80% Spec.	85% Spec.	90% Spec.	95% Spec.	P †
Thickness						
Global	0.82 (0.76, 0.88)	0.74	0.71	0.62	0.52	
N	0.73 (0.66, 0.80)	0.54	0.48	0.46	0.40	
IN	0.82 (0.75, 0.87)	0.74	0.69	0.67	0.57	
IT	0.80 (0.73, 0.86)	0.64	0.58	0.52	0.51	
ST	0.75 (0.68, 0.83)	0.60	0.53	0.51	0.33	
SN	0.81 (0.74, 0.87)	0.71	0.64	0.59	0.37	
T	0.60 (0.51, 0.68)	0.31	0.27	0.25	0.21	
Capillary Density						
wiCD	0.88 (0.82, 0.92)	0.76	0.74	0.73	0.67	**0.032**
cpCD	0.87 (0.81, 0.91)	0.76	0.7	0.69	0.66	0.059
N	0.81 (0.74, 0.87)	0.70	0.65	0.64	0.52	**0.007**
IN	0.78 (0.71, 0.84)	0.62	0.53	0.51	0.45	0.197
IT	0.81 (0.75, 0.87)	0.68	0.65	0.61	0.56	0.649
ST	0.81 (0.74, 0.86)	0.64	0.59	0.57	0.54	0.155
SN	0.78 (0.72, 0.84)	0.65	0.58	0.57	0.48	0.488
T	0.74 (0.66, 0.81)	0.59	0.47	0.40	0.27	**< 0.001**

AUROC: area under the receiver operating characteristic curve; N: nasal; IN: inferonasal; IT: inferotemporal; ST: superotemporal; SN: superonasal; T: temporal; wiCD: whole image capillary density; cpCD: circumpapillary capillary density.

Metrics are shown as AUROCs with bias corrected 95% confidence intervals (CI) and sensitivities at fixed specificities (Spec.) for each classifier. Significance was determined using a paired bootstrap test.

†Statistical significance for the difference between AUROCs of retinal nerve fiber layer and capillary density.

Bolded P indicates statistically significant difference defined as P< 0.05.